

# AEROFOIL AND WING PITCHING MOMENT COEFFICIENT AT ZERO ANGLE OF ATTACK DUE TO DEPLOYMENT OF TRAILING-EDGE SPLIT FLAPS AT LOW SPEEDS

## 1. NOTATION AND UNITS

|                          |  | <i>SI</i> | <i>British</i> |
|--------------------------|--|-----------|----------------|
| $A$                      | aspect ratio, $2s/\bar{c}$   |           |                |
| $C_L$                    | lift coefficient; (lift)/ $qc$ for aerofoil, (lift)/ $qS$ for wing   |           |                |
| $C_{L0}$                 | lift coefficient at zero angle of attack for aerofoil, based on $c$  |           |                |
| $\Delta C_{L0t}$         | increment in lift coefficient at zero angle of attack due to deployment of trailing-edge split flap on aerofoil, based on $c$  |           |                |
| $C_m$                    | pitching moment coefficient; (pitching moment)/ $qc^2$ for aerofoil, (pitching moment)/ $qS\bar{c}$ for wing, referenced to $c/4$ for aerofoil and $\bar{c}/4$ for wing, see Sketch 1.1  |           |                |
| $C_{m\alpha 0}$          | pitching moment coefficient at zero angle of attack for aerofoil, based on $c^2$ and referenced to $c/4$   |           |                |
| $C_{mw\alpha 0}$         | pitching moment coefficient at zero angle of attack for wing, based on $S\bar{c}$ and referenced to $\bar{c}/4$ , see Sketch 1.1   |           |                |
| $\Delta C_{mt\alpha 0}$  | increment in pitching moment coefficient at zero angle of attack due to deployment of trailing-edge split flap on aerofoil, based on $c^2$ and referenced to $c/4$ , see Equation (3.1)  |           |                |
| $\Delta C_{mtw\alpha 0}$ | increment in pitching moment coefficient at zero angle of attack due to deployment of trailing-edge split flap on wing, based on $S\bar{c}$ and referenced to $\bar{c}/4$ , see Equation (3.4)                                   |           |                |
| $c$                      | basic (plain) aerofoil chord ( <i>i.e.</i> chord with high-lift devices undeployed), see Sketch 1.2  | m         | ft             |
| $\bar{c}$                | wing geometric mean chord  | m         | ft             |
| $\bar{\bar{c}}$          | wing aerodynamic mean chord  | m         | ft             |
| $c_r$                    | wing root chord  | m         | ft             |
| $c_t$                    | chord of trailing-edge split flap, see Sketch 1.2  | m         | ft             |
| $h_2$                    | centre of incremental lift at zero angle of attack due to trailing-edge split flap deflection on aerofoil section expressed as fraction of chord, measured positive aft from aerofoil quarter-chord position, see Equation (3.2) |           |                |

|                  |  |                  |                     |
|------------------|--|------------------|---------------------|
| $h_{2T}$         | theoretical value of $h_2$ , see Equation (3.3)  |                  |                     |
| $K_f$            | flap type correlation factor   |                  |                     |
| $K_{f\Lambda}$   | flap type correlation factor for sweep   |                  |                     |
| $K$              | part-span factor; pitching moment coefficient increment due to part-span trailing-edge split flaps extending symmetrically from wing centre-line of unswept wing ( $\Lambda_{1/4} = 0$ ) divided by pitching moment coefficient increment due to full-span trailing-edge split flaps at same deflection angle and wing angle of attack |                  |                     |
| $K_i$            | value of $K$ corresponding to $\eta = \eta_i$ , Figure 1   |                  |                     |
| $K_o$            | value of $K$ corresponding to $\eta = \eta_o$ , Figure 1   |                  |                     |
| $K_\Lambda$      | wing sweep factor dependent on wing taper ratio and spanwise extent of trailing-edge flap, Equation (3.5)  |                  |                     |
| $K_{\Lambda i}$  | value of $K_\Lambda$ corresponding to $\eta = \eta_i$ , Figure 2   |                  |                     |
| $K_{\Lambda o}$  | value of $K_\Lambda$ corresponding to $\eta = \eta_o$ , Figure 2   |                  |                     |
| $M$              | free-stream Mach number  |                  |                     |
| $q$              | free-stream kinetic pressure   | N/m <sup>2</sup> | lbf/ft <sup>2</sup> |
| $R_c$            | aerofoil Reynolds number based on free-stream conditions and $c$   |                  |                     |
| $R_{\bar{c}}$    | wing Reynolds number based on free-stream conditions and $\bar{c}$   |                  |                     |
| $S$              | wing planform area, $2s\bar{c}$  | m <sup>2</sup>   | ft <sup>2</sup>     |
| $s$              | wing semispan, see Sketch 1.1  | m                | ft                  |
| $t$              | maximum thickness of aerofoil  | m                | ft                  |
| $z_{lm}$         | lowest surface ordinate of basic aerofoil, see Sketch 1.2  | m                | ft                  |
| $\delta_t^\circ$ | deflection of trailing-edge flap, positive trailing-edge down, see Sketch 1.2  | deg              | deg                 |
| $\eta$           | spanwise distance from wing centre-line as fraction of semispan  |                  |                     |
| $\eta_i$         | value of $\eta$ at inboard limit of flap, see Sketch 1.1   |                  |                     |
| $\eta_o$         | value of $\eta$ at outboard limit of flap, see Sketch 1.1  |                  |                     |

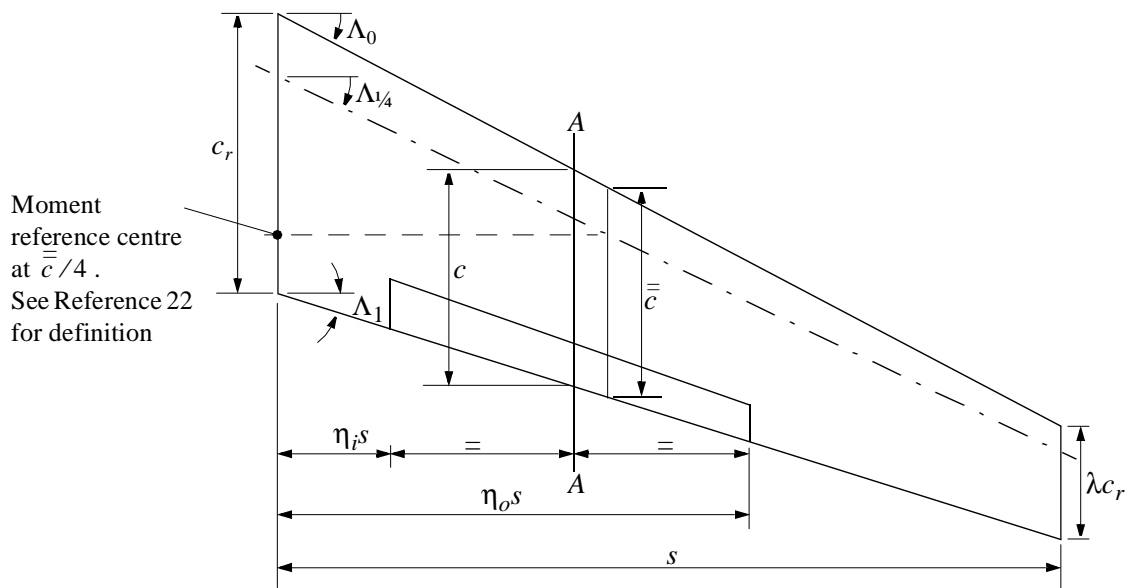
|                 |  |     |     |
|-----------------|--|-----|-----|
| $\Lambda_0$     | wing leading-edge sweep angle, see Sketch 1.1  | deg | deg |
| $\Lambda_{1/4}$ | wing quarter-chord sweep angle, see Sketch 1.1 | deg | deg |
| $\Lambda_1$     | wing trailing-edge sweep angle, see Sketch 1.1 | deg | deg |
| $\lambda$       | wing taper ratio (tip chord/root chord)        |     |     |

### Subscripts

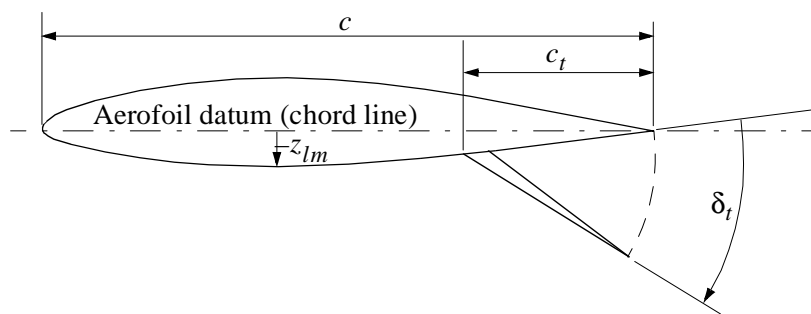
$\alpha_0$  denotes value at zero angle of attack

$( )_{expt}$  denotes experimental value

$( )_{pred}$  denotes predicted value



Sketch 1.1 Wing notation (flaps undeveloped)



Sketch 1.2 Deployed split flap notation (at Section AA)

## 2. INTRODUCTION

This Item provides a method to obtain the increment in pitching moment coefficient at zero angle of attack, due to deployment of trailing-edge split flaps, either on an aerofoil or on a wing.

For aerofoils the method predicts the centre of lift position,  $h_2$ , due to split flap deployment, based on the thin aerofoil theory of Derivation 19 and modified to obtain correlation with the experimental data of Derivations 5, 6, 12 and 17. This is combined with the increment in aerofoil lift coefficient calculated from Item No. 94029 (Derivation 1) to estimate the pitching moment coefficient increment.

For wings with full-span trailing-edge split flaps, factors, dependent on planform geometry, are applied to the pitching moment coefficient increment on an aerofoil section that is representative of the wing, to allow for three-dimensional effects. For wings with part-span trailing-edge flaps, additional factors are introduced that are dependent on the wing taper ratio, aspect ratio and sweep as well as on the spanwise extent of the flap. Derivations 20 and 21 were used as the basis for three dimensional effects, with some adjustment to the simple theoretical assumptions.

Section 3 describes the prediction method and Section 4 discusses Mach number and Reynolds number effects. The accuracy and applicability of the method are addressed in Section 5. The Derivation and References are given in Section 6. Section 7 presents a worked example that illustrates the steps of the calculation.

## 3. PREDICTION METHOD

The method of this Item requires the use of Item No. 94029 to determine the lift increment characteristics of the aerofoil/trailing-edge split-flap combination.

For a wing the *streamwise* section and trailing-edge split flap geometries and angles at the mid-span of the flap panel are taken to be representative of the wing/split-flap system, see Sketches 1.1 and 1.2. By this means the effects of spanwise variation are averaged out. Empirical corrections allow for the effects of wing planform geometry and the spanwise extent of the flaps.

### 3.1 Aerofoil Pitching Moment Coefficient Increment, $\Delta C_{mt\alpha 0}$

The increment in the pitching moment coefficient at zero angle of attack, for deployment of a split flap on an aerofoil is

$$\Delta C_{mt\alpha 0} = -\Delta C_{L0t} h_2 \quad (3.1)$$

where  $\Delta C_{L0t}$  is the increment in lift coefficient at zero angle of attack due to deployment of a split flap on an aerofoil and is obtained from the method of Item No. 94029.

The centre of the lift increment, at zero angle of attack,  $h_2$ , derived empirically for a split flap deflected on an aerofoil section, expressed as a ratio of the chord and measured positive aft from the quarter-chord point, is given by

$$h_2 = h_{2T} - 0.025 + 0.22(c_f/c)^2 - 0.0000457(c_f/c)(\delta_t^\circ)^2 - 0.0436(c_f/c)(z_{lm}/c)\delta_t^\circ \quad (3.2)$$

where  $c_f/c$  is the ratio of the flap chord to the aerofoil chord,

$\delta_i^\circ$  is the flap deflection angle in degrees,

$z_{lm}/c$  is the ratio of the lowest surface ordinate to the aerofoil chord as in Sketch 1.2

and  $h_{2T}$  is the theoretical value of  $h_2$  for a hinged plate on a thin aerofoil from Derivation 19 and is given by

$$h_{2T} = 0.25[1 - (2c_f/c - 1)^2]^{1/2}[1 - (2c_f/c - 1)] / \{\pi - \cos^{-1}(2c_f/c - 1) + [1 - (2c_f/c - 1)^2]^{1/2}\}. \quad (3.3)$$

### 3.2 Wing Pitching Moment Coefficient Increment, $\Delta C_{mtw\alpha 0}$

For a wing at zero angle of attack the increment in pitching moment coefficient due to split flap deployment is

$$\Delta C_{mtw\alpha 0} = K_f (K_o - K_i) \Delta C_{mt\alpha 0} + K_{f\Lambda} [(K_{\Lambda o} - K_{\Lambda i})(A/2) \Delta C_{L0t} \tan \Lambda_{1/4}] \quad (3.4)$$

where  $K_i$  and  $K_o$ , the part-span wing factors, are obtained from Figure 1 as functions of the inboard and outboard limits of the trailing-edge split flap,  $\eta_i$  and  $\eta_o$  respectively, and the taper ratio,  $\lambda$ . Note that  $K_o$  has been modified from the theory of Derivation 20 to improve correlation.

The flap type correlation factors for split flaps have been derived from the data of Derivations 2 to 4, 7 to 11, 13 to 16 and 18 to be  $K_f = 1.0$  and  $K_{f\Lambda} = \cos \Lambda_{1/4}$ ,

$A$  is the wing aspect ratio

and  $K_{\Lambda i}$  and  $K_{\Lambda o}$ , the wing sweep factors, are obtained for part-span split flaps from Figure 2, as functions of the inboard and outboard limits of the trailing-edge split flap,  $\eta_i$  and  $\eta_o$  respectively, and the taper ratio,  $\lambda$ . Note that for all cases for a full-span split flap and for all wings with an unswept quarter-chord line the second term in Equation (3.4) has a value of zero.

The data for  $K_{\Lambda}$  given in Figure 2 were obtained from Derivation 20, in the simplified form

$$K_{\Lambda} = \frac{\eta(1 - \eta)[(1 + 2\lambda) - \eta(1 - \lambda^2)]}{4(1 + \lambda + \lambda^2)}. \quad (3.5)$$

## 4. EFFECTS OF MACH NUMBER AND REYNOLDS NUMBER

### 4.1 Mach Number Effects

High local Mach numbers will occur at low free-stream Mach number as a result of high angle deployment of trailing-edge split flaps. Significant Mach number effects will occur at free-stream Mach numbers greater than about 0.2. None of the data considered for this Item was for a Mach number greater than 0.2.

### 4.2 Reynolds Number Effects

For the data used in the derivation of this Item no effect of Reynolds number on  $\Delta C_{mt\alpha 0}$  or  $\Delta C_{mtw\alpha 0}$  was found over the ranges of Reynolds number shown in Tables 5.1 and 5.2.

5. APPLICABILITY AND ACCURACY

5.1 Applicability

5.1.1 Aerofoils

The method given in this Item for estimating the position of the centre of the lift increment and of the increment in pitching moment coefficient at zero angle of attack, due to deployment of a trailing-edge split flap, applies only to aerofoils without the deployment of a leading-edge device and with no chord extension.

Table 5.1 summarises the parameter ranges covered by the experimental data, obtained from Derivations 5, 6, 12 and 17, from which Equation (3.2) was derived to obtain correlation.

**TABLE 5.1 Parameter ranges for experimental data for trailing-edge split flaps on aerofoils used in the method of Section 3.1**

| <i>Parameter</i>     | <i>Range</i>     |
|----------------------|------------------|
| $t/c$                | 0.06 to 0.30     |
| $z_{lm}/c$           | -0.019 to -0.135 |
| $c_f/c$              | 0.1 to 0.4       |
| $\delta_t^\circ$     | 0 to 90°         |
| $R_c \times 10^{-6}$ | 2.0 to 6.0       |
| $M$                  | 0.11 to 0.17     |

5.1.2 Wings

The method given in this Item for estimating the increment in pitching moment coefficient, at zero angle of attack, due to deployment of a trailing-edge split flap on a wing, has been shown to be applicable to straight-tapered wings covering a wide range of planform parameters. Table 5.2 summarises the parameter ranges that were used in the development of the method. Note that the method should apply to the full range of chord ratios and flap angles in Table 5.1.

For a wing where  $c_f/c$  is not constant, the flap should be divided into several equal spanwise portions, calculation made for each and the results summed to provide a total value of  $\Delta C_{m_{tw}\alpha_0}$ . The number of portions required will depend on how rapidly the ratio  $c_f/c$  varies across the span.

No wings with cranked leading or trailing edges or curved tips were included in the analysis. It is suggested that for such wings the planform parameters,  $\lambda$  and  $\Lambda_{1/4}$ , for the purposes of Figures 1 and 2 and for use in Equation (3.4) and for the estimation of  $K_f$  and  $K_{f\Lambda}$ , be calculated for the equivalent straight-tapered planform as defined in Item No. 76003 (Reference 22). Care should be taken with the definition of  $c_f/c$  and the user of the final result should be aware of the non-validated use of the method for such wings.

The method has only been validated for wings with no leading-edge devices and with no chord extension due to split flap deployment.

**TABLE 5.2 Parameter ranges for experimental data for trailing-edge split flaps on wings used in the method of Sections 3.2**

| <i>Parameter</i>             | <i>Range</i> |
|------------------------------|--------------|
| $A$                          | 3.4 to 9.0   |
| $A \tan \Lambda_0$           | 0 to 8.5     |
| $A \tan \Lambda_{1/2}$       | 0 to 7.6     |
| $\Lambda_0$                  | 0 to 63°     |
| $\Lambda_1$                  | -12° to 53°  |
| $\lambda$                    | 0.2 to 1.0   |
| $c_t/c$                      | 0.15 to 0.25 |
| $\delta_t^\circ$             | 10° to 75°   |
| $\eta_i$                     | 0 to 0.8     |
| $\eta_o$                     | 0.2 to 1.0   |
| $R_{\bar{c}} \times 10^{-6}$ | 0.6 to 7.0   |
| $M$                          | $\leq 0.2$   |

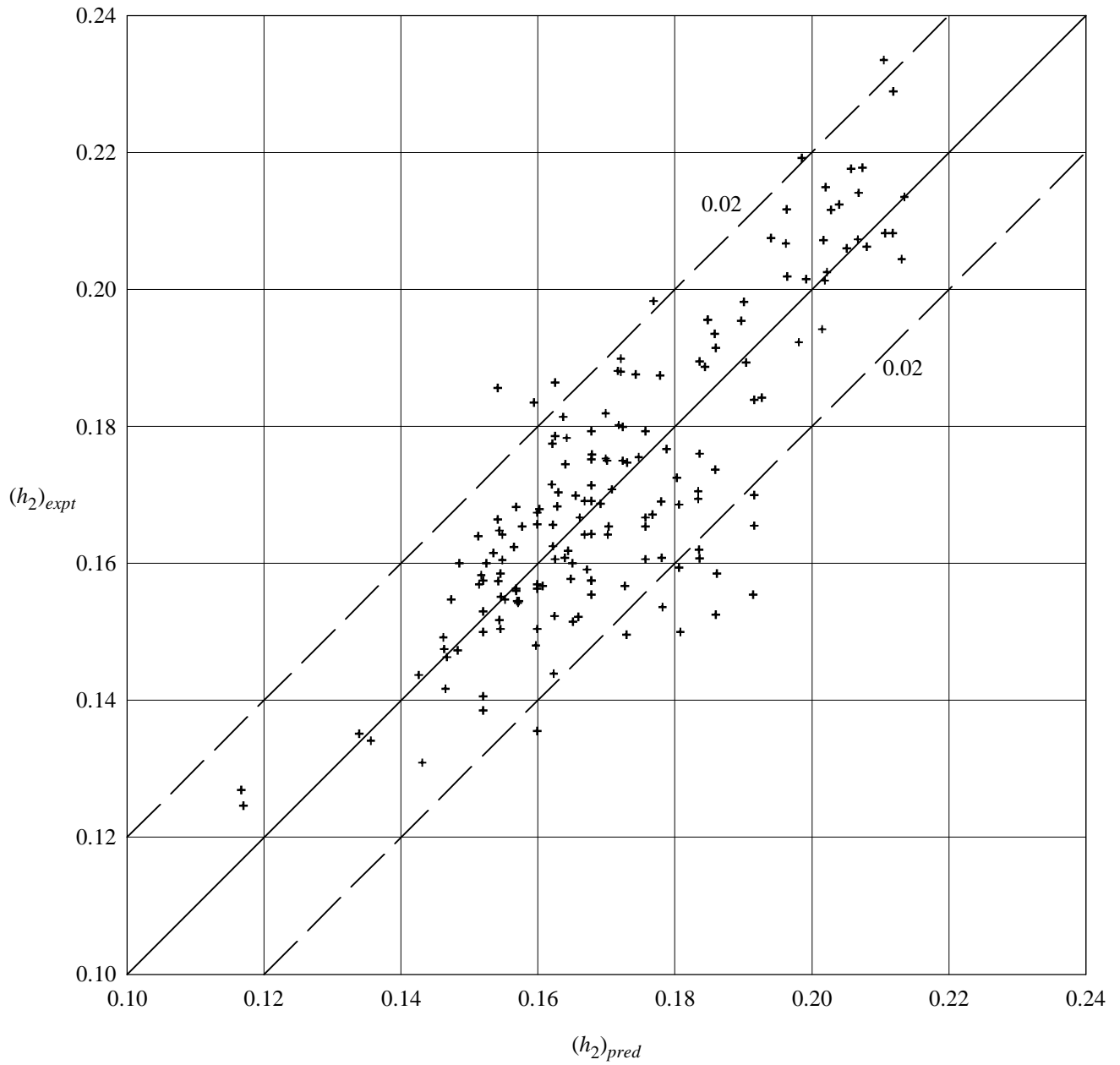
## 5.2 Accuracy

### 5.2.1 Aerofoils

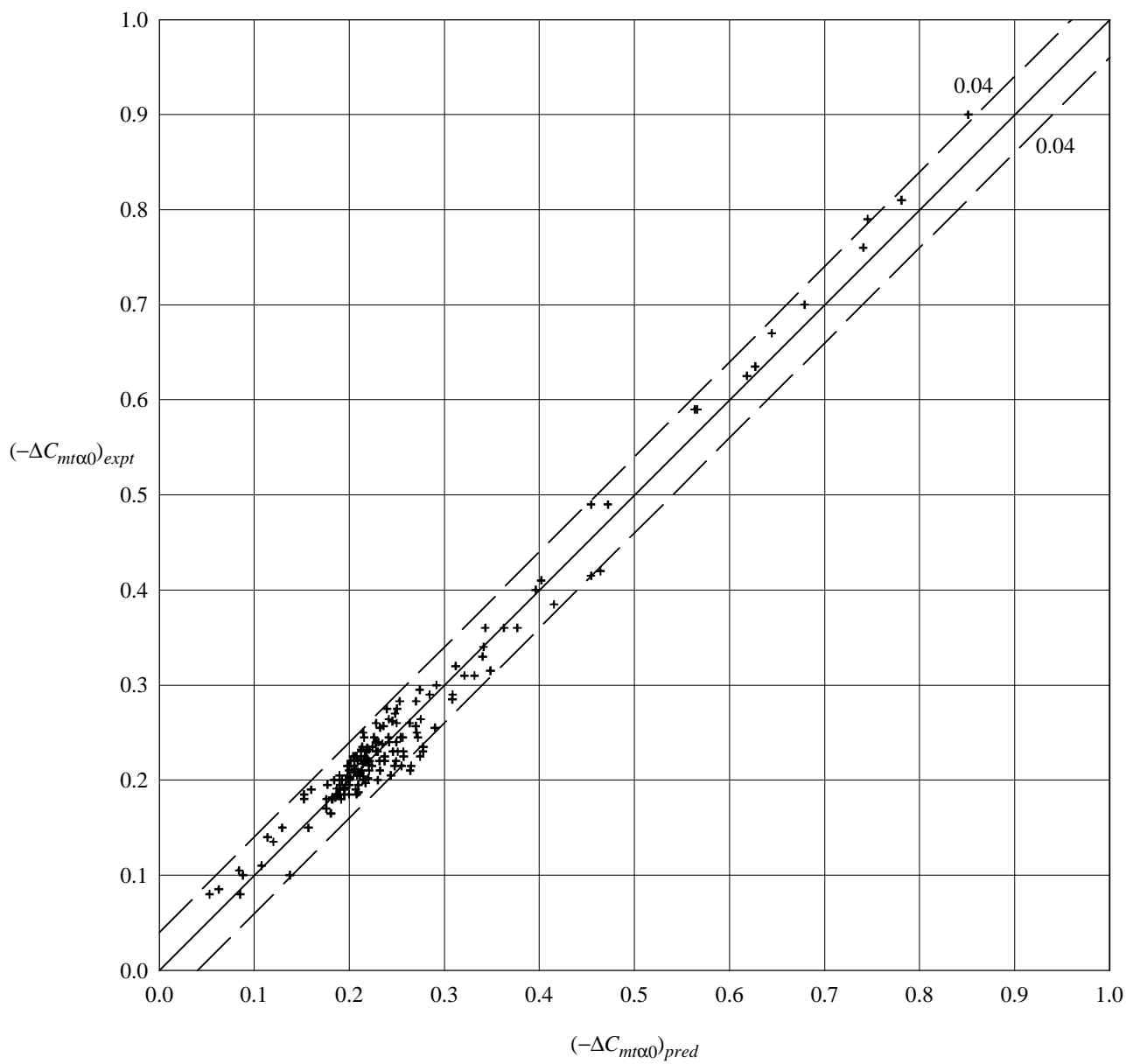
Sketch 5.1 shows the comparison between predicted and experimental values of the centre of the lift increment,  $h_2$ , due to deployment of trailing-edge split flaps on an aerofoil, for data from Derivations 5, 6, 12 and 17; 92% of the data for  $h_2$  are correlated to within  $\pm 0.02$ . Sketch 5.2 shows the corresponding comparison between predicted and experimental values of pitching moment coefficient increments; 95% of the data are correlated to within  $\pm 0.04$ .

### 5.2.2 Wings

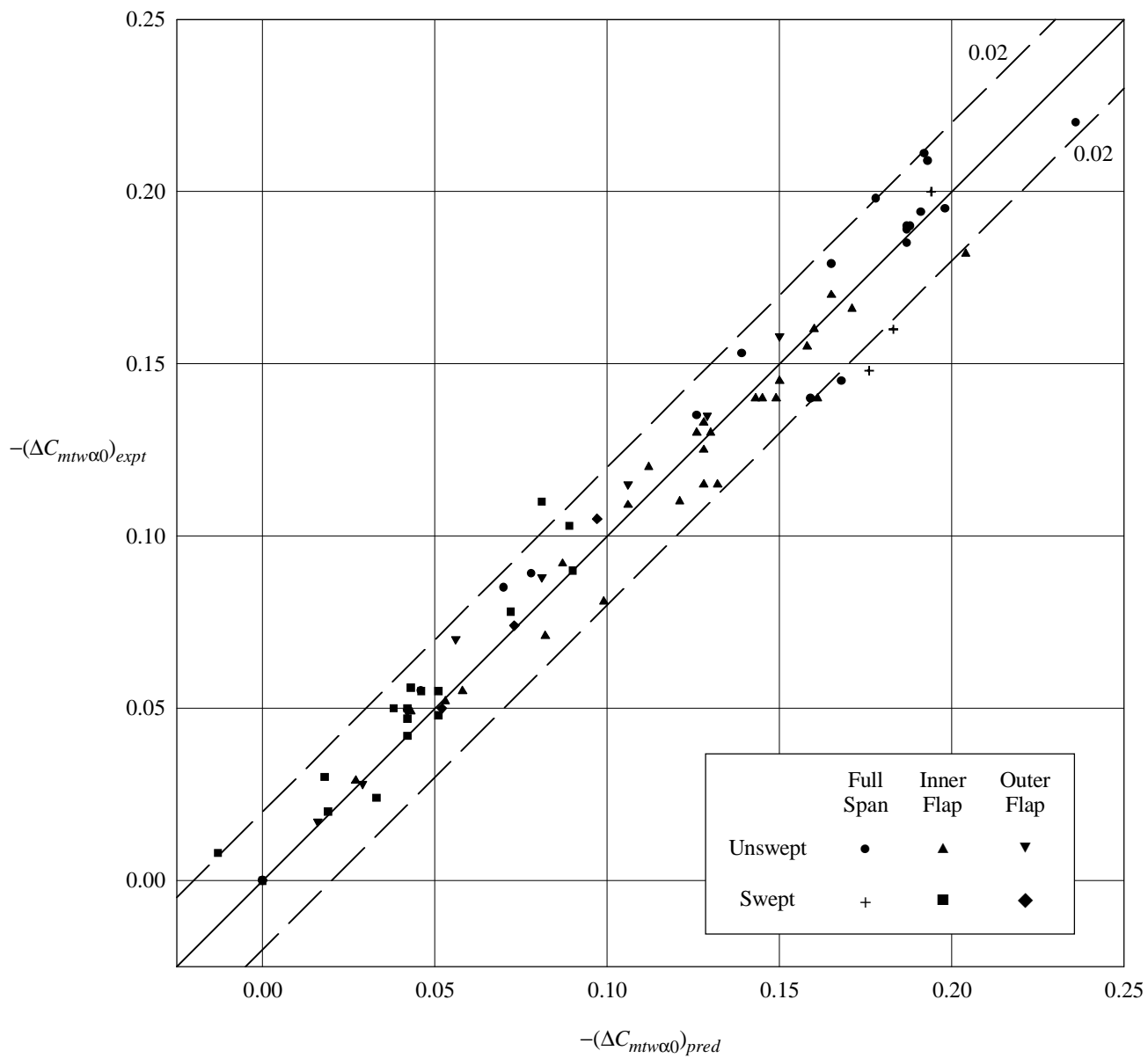
Sketch 5.3 shows the comparison between predicted and experimental values of the pitching moment coefficient increment,  $\Delta C_{mtw\alpha 0}$ , due to deployment of both full-span and part-span trailing-edge split flaps on unswept wings and on swept wings, for data from Derivations 2 to 4, 7 to 11, 13 to 16 and 18; 92% of the data points are within  $\pm 0.02$  and the rms error is 0.011.



Sketch 5.1 Comparison of predicted and experimental values of  $h_2$



Sketch 5.2 Comparison of predicted and experimental values of  $\Delta C_{m\alpha_0}$



**Sketch 5.3 Comparison of predicted and experimental values of  $\Delta C_{mtw\alpha_0}$**

## 6. DERIVATION AND REFERENCES

### 6.1 Derivation

The Derivation lists selected sources of information that have been used in the preparation of this Item.

#### 6.1.1 ESDU Data Items

1. ESDU Increments in aerofoil lift coefficient at zero angle of attack and in maximum lift coefficient due to deployment of a trailing-edge split flap, with or without a leading-edge high-lift device at low speeds.  
ESDU International, Item No. 94029, 1994.

#### 6.1.2 Wind-tunnel test reports

2. WENZINGER, C.J. The effect of partial-span split flaps on the aerodynamic characteristics of a Clarke Y wing.  
NACA tech. Note 472, 1933.
3. WENZINGER, C.J. The effects of full-span and partial-span split flaps on the aerodynamic characteristics of a tapered wing.  
NACA tech. Note 505, 1934.
4. WENZINGER, C.J. Wind-tunnel investigation of tapered wings with ordinary ailerons and partial span split flaps.  
NACA Rep. 611, 1937.
5. WENZINGER, C.J.  
HARRIS, T.A. Wing-tunnel investigation of NACA 23012, 23021 and 23030 airfoils with various sizes of split flap.  
NACA Rep. 668, 1939.
6. FULLMER, F.F. Wind-tunnel investigation of NACA 66(215)-216, 66,1-212 and 65<sub>1</sub>-212 airfoils with 0.2-airfoil-chord split flaps.  
NACA WR L-140, 1944.
7. McCORMACK, G.M.  
STEVENS, V.I. An investigation of the low speed stability and control characteristics of swept forward and sweptback wings in the Ames 40- by 80- foot wind-tunnel.  
NACA RM A6K15 (TIL 1362), 1947.
8. SIVELLS, J.C.  
SPOONER, S.H. Investigation in the Langley 19-foot pressure tunnel of two wings of NACA 65-210 and 64-210 airfoil sections with various types of flaps.  
NACA Rep. 942, 1947.
9. CONNER, D.W.  
NEELY, R.H. Effects of a fuselage and various high-lift and stall control flaps on aerodynamic characteristics in pitch of an NACA 64-series 40° sweptback wing.  
NACA RM L6L27 (TIL 1375), 1947.
10. GRAHAM, R.R. Investigation of high-lift and stall control devices on a NACA 64-series 42° sweptback wing with and without a fuselage.  
NACA RM L7G09 (TIL 1407), 1947.

11. LANGE, R.H.  
MAY, R.W. Effect of leading-edge high-lift devices and split flaps on the maximum lift and lateral characteristics of a rectangular wing of aspect ratio 3.4 with circular arc airfoil sections at Reynolds numbers from  $2.9 \times 10^6$  to  $8.4 \times 10^6$ .  
NACA RM L8D30 (TIL 1971), 1948.
12. ABBOTT, I.H.  
GREENBURG, H. Tests in the variable-density wind-tunnel of the NACA 23012 airfoil with plain and split flaps.  
NACA Rep. 661, 1949.
13. HOPKINS, E.J. Aerodynamic study of a wing-fuselage combination, employing a wing swept back  $63^\circ$ : effects of split flaps, elevons, and leading-edge devices at low speed.  
NACA RM A9C21 (TIL 2127), 1949.
14. SALMI, R.J. Effects of leading-edge device and trailing-edge flaps on longitudinal characteristics of two  $47.7^\circ$  sweptback wings of aspect ratio 5.1 and 6 at a Reynolds number of  $6.0 \times 10^6$ .  
NACA RM L50F20 (TIL 2466), 1950.
15. PRATT, G.L.  
SHEILDS, R.R. Low speed longitudinal characteristics of a  $45^\circ$  sweptback wing of aspect ratio 8 with high-lift and stall control devices at Reynolds numbers from 1,500,400 to 4,800,000.  
NACA RM L51J04 (TIL 3038), 1952.
16. LICHTENSTEIN, J.H.  
WILLIAMS, J.L. Effect of high-lift devices on the static-lateral-stability derivatives of a  $45^\circ$  sweptback wing of aspect ratio 4.0 and taper ratio 0.6 in combination with a body.  
NACA tech. Note 2819, 1952.
17. ABBOTT, I.H.  
VON DOENHOFF, A.E. *Theory of Wing Sections*.  
Dover Publications, New York, 1959.
18. MORGAN, H.L.  
PAULSON, J.W. Aerodynamic characteristics of wing-body configuration with two advanced general aviation airfoil sections and simple flap systems.  
NASA tech. Note D-8524, 1977.

### 6.1.3 Theory

19. GLAUERT, H. Theoretical relationships for an aerofoil with hinged flap.  
ARC R&M 1095, 1927.
20. DENT, M.M.  
CURTIS, M.F. A method of estimating the effect of flaps on pitching moment and lift on tailless aircraft.  
RAE Report No. Aero 1861, 1943.
21. YOUNG, A.D. The aerodynamic characteristics of flaps.  
ARC R&M 2622, (RAE Report No. Aero 2185), 1947.

## 6.2 References

The References list selected sources of information supplementary to that given in this Item.

22. ESDU Geometrical properties of cranked and straight tapered wing planforms. ESDU International, Item No. 76003, 1976.
23. ESDU Wing lift coefficient increment at zero angle of attack due to deployment of trailing-edge split flaps at low speeds. ESDU International, Item No. 97009, 1997.

7. EXAMPLE

Estimate the increment in pitching moment coefficient at zero angle of attack for a Reynolds number  $R_{\bar{c}} = 7 \times 10^6$  and a free-stream Mach number  $M = 0.2$  for the wing with a part-span trailing-edge split flap shown in Sketch 7.1. The wing has the planform parameter values

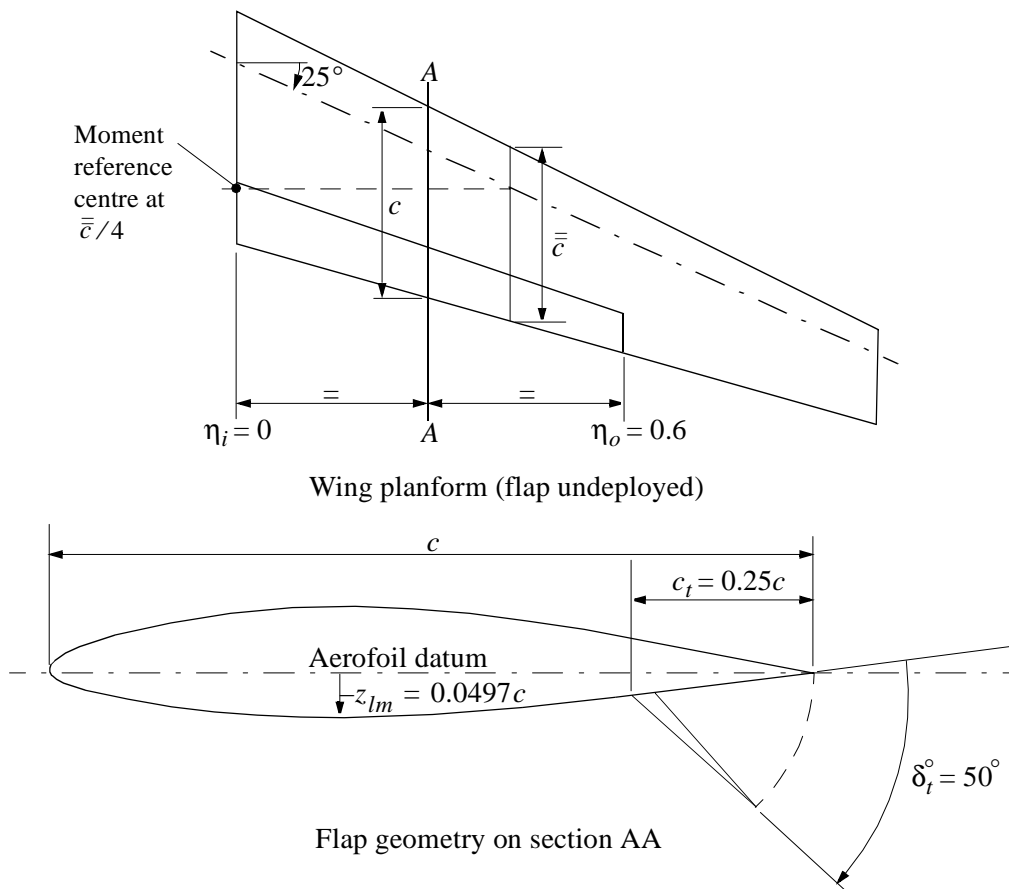
$$A = 8, \Lambda_{1/4} = 25^\circ \text{ and } \lambda = 0.4$$

and across the span, the constant section, NACA 63<sub>1</sub>-212, for which

$$z_{lm}/c = -0.0497.$$

The flap extends from the wing centre-line to 60% of the wing semispan. The location of the flap hinge-line is a constant proportion (75%) of the local wing chord. The required streamwise geometrical parameters for the flap are

$$c_f/c = 0.25, \delta_t^\circ = 50^\circ.$$



Sketch 7.1

(1) **Determine  $\Delta C_{L0t}$**

Note that this example is for the same geometry as the example given in Item No. 97009 (Reference 23) to illustrate the derivation of the value of the increment in lift coefficient at zero angle of attack,  $\Delta C_{L0tw}$ . To avoid repetition the value of  $\Delta C_{L0t}$  required for this example is taken from Item No 97009, in which

$$\Delta C_{L0t} = 1.237.$$

Also from the example of Item 97009 the sweep angles  $\Lambda_0 = 27.5^\circ$  and  $\Lambda_1 = 17^\circ$  and the parameter  $A \tan \Lambda_0 = 4.16$  all lie within the ranges shown on Table 5.2.

(2) **Determine  $h_2$**

From Equation (3.3)

$$\begin{aligned} h_{2T} &= 0.25[1 - (2c_t/c - 1)^2]^{1/2}[1 - (2c_t/c - 1)]/\{\pi - \cos^{-1}(2c_t/c - 1) + [1 - (2c_t/c - 1)^2]^{1/2}\} \\ &= 0.25[1 - (2 \times 0.25 - 1)^2]^{1/2}[1 - (2 \times 0.25 - 1)]/\{\pi - \cos^{-1}(2 \times 0.25 - 1) + [1 - (2 \times 0.25 - 1)^2]^{1/2}\} \\ &= 0.25[1 - (-0.5)^2]^{1/2} \times [1 - (-0.5)]/\{3.142 - \cos^{-1}(-0.5) + [1 - (-0.5)^2]^{1/2}\} \\ &= 0.25 \times 0.866 \times 1.5/\{3.142 - 2.094 + 0.866\} \\ &= 0.1697. \end{aligned}$$

From Equation (3.2)

$$\begin{aligned} h_2 &= h_{2T} - 0.025 + 0.22(c_t/c)^2 - 0.0000457(c_t/c)(\delta_t^\circ)^2 - 0.0436(c_t/c)(z_{lm}/c)\delta_t^\circ \\ &= 0.1697 - 0.025 + 0.22 \times (0.25)^2 - 0.0000457 \times 0.25 \times 50^2 - 0.0436 \times 0.25 \times (-0.0497) \times 50 \\ &= 0.1697 - 0.025 + 0.0138 - 0.0286 + 0.0271 \\ &= 0.1570. \end{aligned}$$

(3) **Determine  $\Delta C_{mt\alpha 0}$**

From Equation (3.1)

$$\begin{aligned} \Delta C_{mt\alpha 0} &= -\Delta C_{L0t} h_2 \\ &= -1.237 \times 0.1570 \\ &= -0.1942. \end{aligned}$$

(4) **Determine  $\Delta C_{mtw\alpha 0}$**

From Equation (3.4)

$$\Delta C_{mtw\alpha 0} = K_f (K_o - K_i) \Delta C_{mt\alpha 0} + K_{f\Lambda} [(K_{\Lambda o} - K_{\Lambda i})(A/2) \Delta C_{L0t} \tan \Lambda_{1/4}]$$

From Figure 1 for  $\eta_i = 0$  and  $\lambda = 0.4$

$$K_i = 0$$

and for  $\eta_o = 0.6$

$$K_o = 0.79.$$

From Figure 2 for  $\eta_i = 0$  and  $\lambda = 0.4$

$$K_{\Lambda i} = 0$$

and for  $\eta_o = 0.6$

$$K_{\Lambda o} = 0.0498.$$

Also  $K_f = 1.0$

$$\begin{aligned} \text{and } K_{f\Lambda} &= \cos \Lambda_{1/4} \\ &= \cos 25^\circ \\ &= 0.9063. \end{aligned}$$

Hence

$$\begin{aligned} \Delta C_{mtw\alpha 0} &= 1.0 \times (0.79 - 0.0) \times (-0.1942) + 0.9423 \times 0.9063 \times [(0.0498 - 0.0) \times 8/2 \times 1.237 \times \tan 25^\circ] \\ &= -0.79 \times 0.1942 + 0.9423 \times 0.9063 \times 0.0498 \times 4 \times 1.237 \times 0.4663 \\ &= -0.1534 + 0.1041 \\ &= -0.0493 \\ &\approx -0.049. \end{aligned}$$

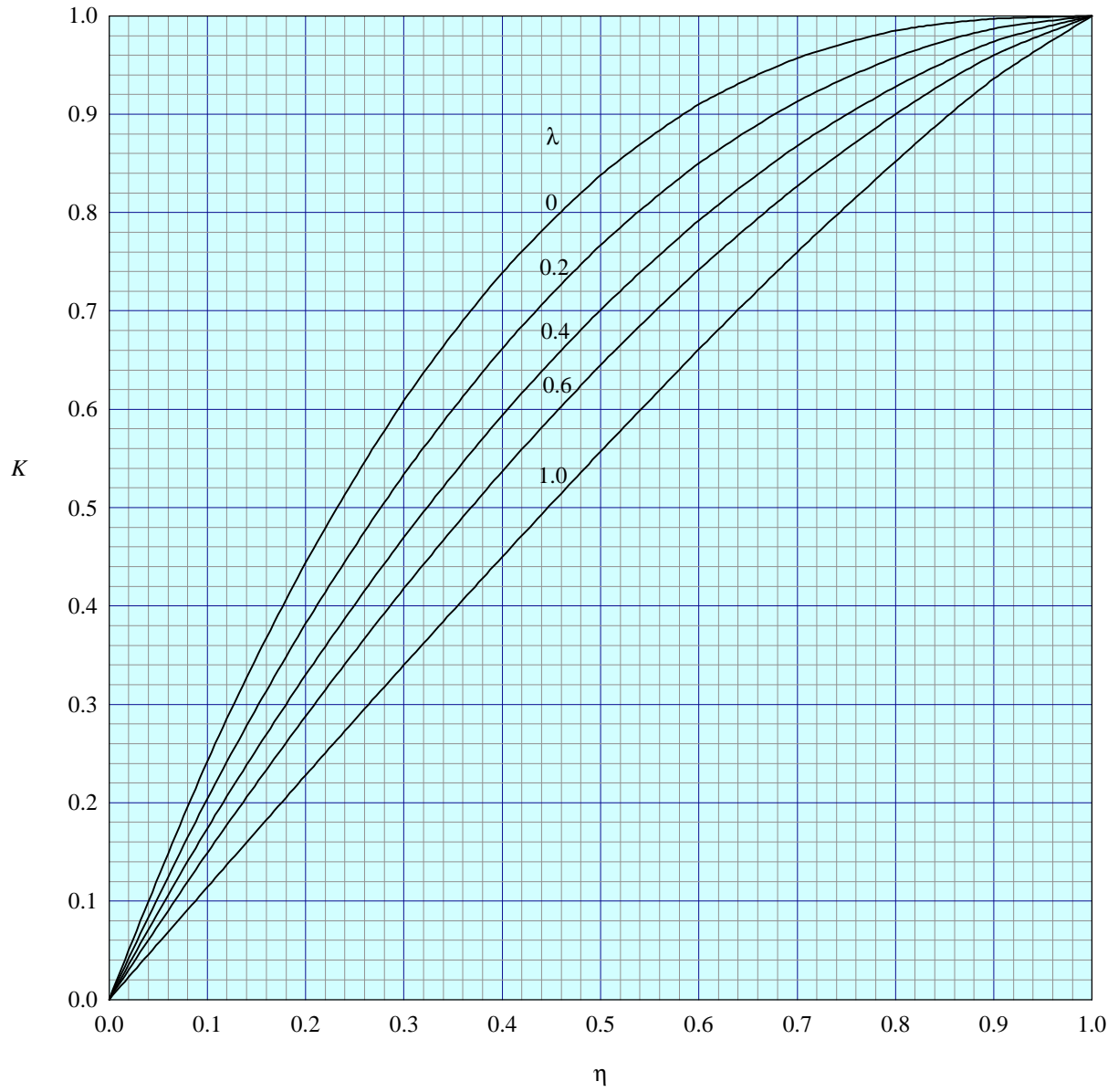


FIGURE 1 PART-SPAN FACTOR,  $K$ , FOR SPLIT FLAPS

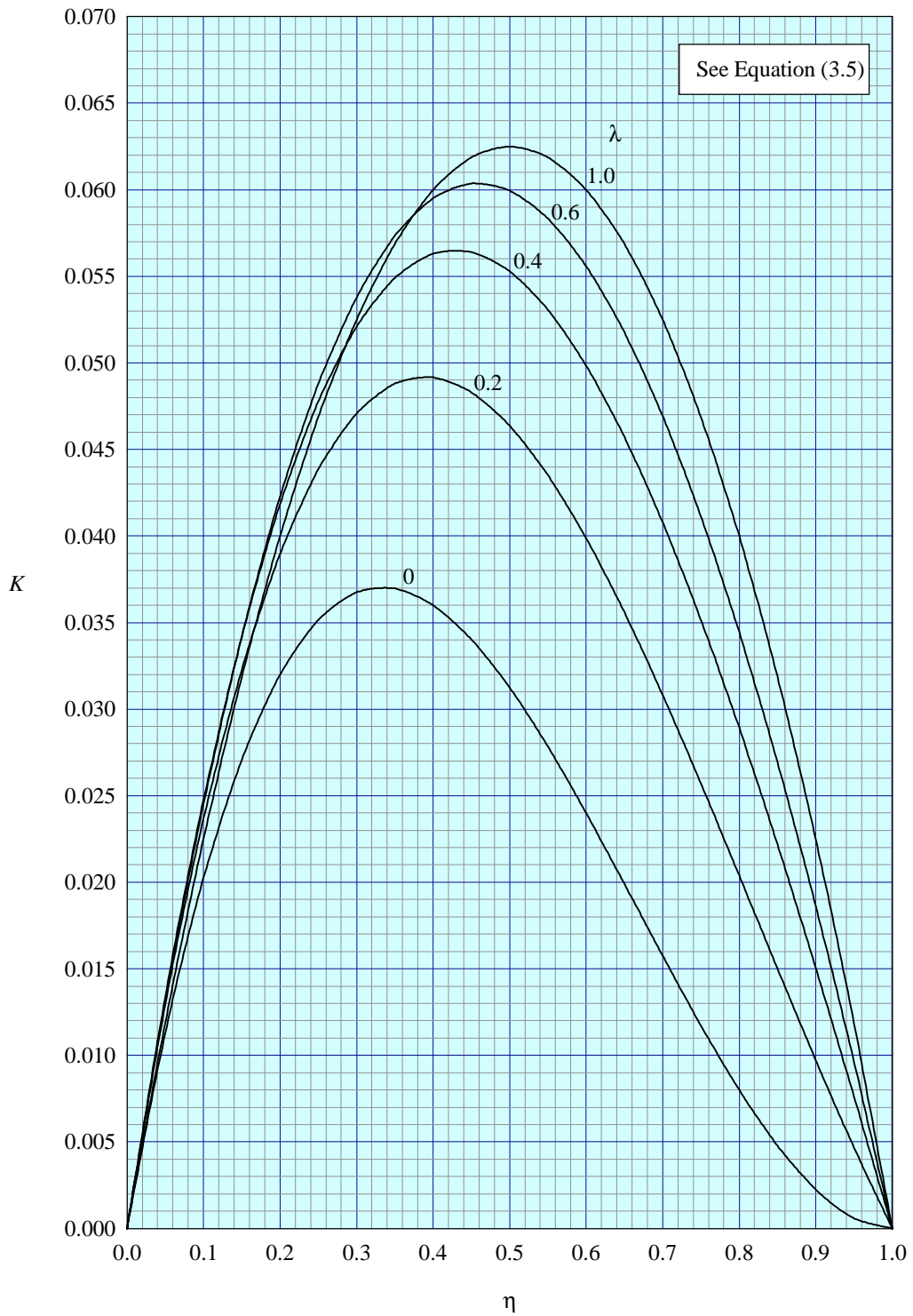


FIGURE 2 PART-SPAN FACTOR,  $K_{\Lambda}$ , FOR SPLIT FLAPS

## THE PREPARATION OF THIS DATA ITEM

The work on this particular Data Item, which supersedes in part Item Nos Aero F.08.01.01 and F.08.01.02, was monitored and guided by the Aerodynamics Committee, which first met in 1942 and now has the following membership:

### Chairman

Mr H.C. Garner – Independent

### Members

Dr M.Z. Bouter\* – Raytheon Aircraft Co., Wichita, Kansas, USA  
Mr P.D. Chappell – Independent  
Dr P.C. Dexter – British Aerospace plc, Sowerby Research Centre, Bristol  
Mr J.R.J. Dovey – Independent  
Dr K.P. Garry – Cranfield University  
Mr D.H. Graham\* – Northrop Grumman Corp., Pico Rivera, Calif., USA  
Mr M.J. Green – Independent  
Dr H.P. Horton – Queen Mary and Westfield College, University of London  
Dr D.W. Hurst – University of Glasgow  
Mr M. Jager\* – Boeing, Long Beach, Calif., USA  
Mr K. Karling\* – Saab-Scania AB, Linköping, Sweden  
Dr E.H. Kitchen – Rolls Royce plc, Derby  
Miss M. Maina – Aircraft Research Association  
Mr M. Maurel – Aérospatiale, Toulouse, France  
Mr C.M. Newbold – DERA, Farnborough  
Mr J.B. Newton – British Aerospace Defence Ltd, Warton  
Mr M.J. Pow – British Aerospace Airbus Ltd, Filton  
Mr R. Sanderson – Daimler-Benz Aerospace Airbus, GmbH, Bremen, Germany  
Mr J. Tweedie – Short Brothers plc, Belfast  
Mr A.J. Wells – Avro International Aerospace, Woodford

\* Corresponding Member.

The technical work in the assessment of the available information and the development and subsequent construction of the Data Item method was carried out under contract to ESDU by Mr J.R.J. Dovey.